IJIREEICE ISSN (O) 2321-2004, ISSN (P) 2321-5526

International Journal of Innovative Research in Electrical, Electronics, Instrumentation and Control Engineering

Impact Factor 8.021 ⁜ Peer-reviewed & Refereed journal ⁜ Vol. 14, Issue 6, June 2026

DOI: 10.17148/IJIREEICE.2026.14639

Design and Study of a Plastic Optical Fibre-Based Evanescent-Field Biosensor

A.K. SHAHI

Department of Physics, Ram Lalit Singh P.G. College, Kailhat, Narayanpur, U.P. 231305

Abstract: A refractive-index (RI) sensor based on the evanescent-field principle of a declad plastic optical fibre (POF) was designed and experimentally characterized. A section of the polymer cladding of a step-index POF (core RI 1.49, numerical aperture 0.5, 650 µm core diameter, 20 µm cladding thickness) was removed by an acetone/distilled-water de cladding procedure to expose the fibre core to the surrounding medium, converting the medium itself into an effective cladding. Aqueous sodium chloride (NaCl) solutions of increasing weight/volume concentration (0–0.20 %, RI 1.332–1.361) were used as surrogate analytes, chosen because they reproduce the intensity response obtained when a biofilm of Pseudomonas aeruginosa is grown on the exposed core. White light was launched into the fibre and the transmitted spectrum was recorded on a spectrograph interfaced with Avantes acquisition software. The transmitted light intensity was found to increase monotonically with the refractive index of the surrounding solution, and the sensitivity, defined as the change in intensity per unit change in refractive index, reached a maximum of 3.4×10^5 counts/RIU between RI 1.350 and 1.360. The results confirm that a simply prepared, low-cost declad-POF probe can operate as a sensitive intrinsic evanescent-field transducer and provide a viable low-cost platform for optical bio-sensing applications.

Keywords: Plastic optical fibre; Evanescent-field sensor; Refractive-index sensing; Biosensor; Total internal reflection; Decladding.

1. INTRODUCTION

Fibre optics is a technology in which information is converted into optical signals and guided along thin dielectric waveguides — optical fibres — that confine electromagnetic energy to their core and propagate it parallel to the fibre axis. Optical-fibre sensors have progressively bridged the optical-communications and optoelectronics industries: because photons rather than electrons are transported, such sensors are lightweight, immune to electromagnetic interference, and can be safely deployed close to high-voltage or corrosive environments [1].

Glass optical fibre (GOF) sensor technology is well established, but plastic (polymer) optical fibre (POF) sensors have emerged rapidly because of their large core size, large numerical aperture, mechanical flexibility, ruggedness, ease of termination and markedly lower cost, even though POF attenuation restricts practical sensing lengths to tens of metres [9,12]. These properties make POF particularly attractive for short-length, disposable, low-cost sensing probes.

A biosensor, as defined by IUPAC, is a self-contained integrated device that provides quantitative or semi-quantitative analytical information using a biological recognition element held in direct spatial contact with a transducer, distinguishing it from a bioanalytical system that requires additional reagent-processing steps [6]. Depending on the recognition mechanism, biosensors are broadly classified as catalytic (enzyme- or metabolism-based) or affinity (antibody–antigen, nucleic acid, or receptor-based) devices. When the transducer is optical, the fibre may act either as an intrinsic sensor, in which the analyte interacts directly with the guided light within the fibre, or as an extrinsic sensor, in which the fibre merely delivers and collects light from a remote sensing region [3,13].

The present work develops and characterises an intrinsic, evanescent-field POF sensor obtained by locally removing the fibre cladding. Aqueous NaCl solutions of known, tunable refractive index were used as a convenient, stable analogue of the refractive-index change produced by biological growth (e.g. bacterial biofilm) on the exposed core, allowing the intensity response and sensitivity of the transducer to be quantified before biological deployment [2].

2. THEORETICAL BACKGROUND

2.1 Light guidance and total internal reflection

A step-index optical fibre consists of a core of refractive index n1 surrounded by a cladding of lower refractive index n2. Snell's law relates the propagation angles at the core/cladding interface,

$$n1\ sin\theta 1 = n2\ sin\theta 2 \quad (1)$$

 This work is licensed under a Creative Commons Attribution 4.0 International License

International Journal of Innovative Research in Electrical, Electronics, Instrumentation and Control Engineering
Impact Factor 8.021 ⁜ Peer-reviewed & Refereed journal ⁜ Vol. 14, Issue 6, June 2026
DOI: 10.17148/IJIREEICE.2026.14639

and total internal reflection (TIR) occurs when the angle of incidence exceeds the critical angle θc, given by $\sin\theta c = n2/n1$. Light coupled into the fibre within the acceptance cone defined by the numerical aperture,

$$NA = \sin\theta a = \sqrt{(n1^2 - n2^2)}, \quad (2)$$

undergoes TIR at every subsequent core/cladding interaction and is guided along the fibre length [1].

2.2 Modes, attenuation and the evanescent field

Guided light may be classified into meridional rays, which cross the fibre axis at each reflection, and skew rays, which follow a helical path without crossing the axis; skew rays couple proportionally more power into the cladding region and are therefore of particular interest for evanescent-field sensing [1,4]. Although an ideal step-index fibre is loss-free, real fibres attenuate light through absorption, scattering and geometrical (bending) losses; in particular, the refractive index, absorption and scattering properties of the cladding directly govern the fraction of guided power that leaks into the evanescent field outside the core [7]. A fraction of the optical power in a single-mode fibre travels in the cladding as an evanescent wave whose intensity decays exponentially with distance from the core, while multimode fibres additionally support tunnelling rays that extend further into the surrounding medium [2,4].

When the cladding is locally removed, the surrounding medium itself becomes the effective cladding of the fibre. Because the evanescent field decays into whatever material is in contact with the core, any change in the refractive index (or absorption) of that medium modulates the transmitted intensity, forming the basis of the intrinsic evanescent-field sensor used in this work [2,7].

3. OPTICAL-FIBRE BIOSENSOR CLASSIFICATION

Optical-fibre biosensors can be combined with a wide range of spectroscopic modalities — absorbance, fluorescence, phosphorescence, refractive index, luminescence and surface plasmon resonance — and can employ enzymes, antibodies/antigens, nucleic acids, whole cells or biomimetic receptors as the biological recognition element, coupled respectively to electrochemical, optical, mass-sensitive or thermometric transduction (Table 1) [6,13]. Their principal advantages include label-free, real-time detection; immunity to electromagnetic interference; multiplexing capability; miniaturisation; and low fabrication cost, at the expense of some sensitivity to ambient light, photobleaching of immobilised reagents and comparatively long response times for mass-transfer-limited reactions [13]. Replacing GOF with POF further reduces cost and improves fracture toughness, bend tolerance and ease of handling, although at somewhat higher intrinsic attenuation [9,12].

Table 1. Biological recognition elements and corresponding signal-transduction principles used in biosensor design [6].

Recognition element	Signal transducer
Enzymes (catalytic or inhibition-based)	Electrochemical (potentiometric, amperometric, conductance, capacitative)
Antibodies / antigens	Optical (absorbance, reflectance, luminescence, RI, light scattering)
Nucleic acids	Mass-sensitive (piezoelectric, surface acoustic wave)
Whole cells / non-enzymatic proteins	Thermometric (thermistor, pyroelectric, optical, enthalpimeter)
Biomimetic receptors (engineered antibodies, aptamers, MIPs)	—

4. MATERIALS AND METHODS

4.1 Sensing fibre

The sensor probe was fabricated from a step-index POF with core refractive index 1.49, numerical aperture 0.5, 650 µm core diameter and 20 µm Cytop cladding thickness (transmission loss 0.15 dB/m, bandwidth 40 MHz over 50 m, operating range −55 to 85 °C). A short section of the doped Cytop cladding was removed to expose the core to the analyte, converting the analyte into the effective cladding of that region [7,12].

4.2 Decladding procedure

The region of fibre to be declad was clamped to avoid brittle stress fracture. Neat acetone was applied dropwise to the target area until the cladding wrinkled and detached from the core; the loosened cladding was then removed with optical

© IJIREEICE This work is licensed under a Creative Commons Attribution 4.0 International License

International Journal of Innovative Research in Electrical, Electronics, Instrumentation and Control Engineering
Impact Factor 8.021 ⪤ Peer-reviewed & Refereed journal ⪤ Vol. 14, Issue 6, June 2026
DOI: 10.17148/IJIREEICE.2026.14639

tissue soaked in a 2:8 acetone/distilled-water mixture, which halts further dissolution while keeping the cladding pliable enough for removal. The process required approximately 7–8 h. The declad region was rinsed thoroughly with distilled water to remove residual acetone and finally wiped with isopropyl alcohol to yield a clean, grease-free core.

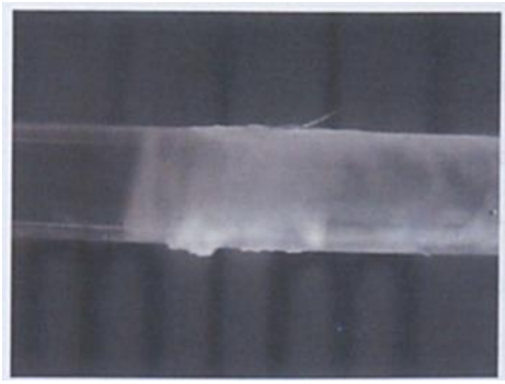

Fig. 1. Declad plastic optical fibre core (left) alongside an intact section with cladding retained (right).

4.3 Preparation of NaCl solutions

Aqueous NaCl solutions of known refractive index were prepared by the weight/volume (w/v) method,

$$\% \ w/v = [\text{mass of solute (g)} / \text{volume of solution (mL)}] \times 100. \quad (3)$$

For example, a 10 % (w/v) solution corresponds to 4.8 g of NaCl dissolved in 30 mL of solution. The weighed NaCl was added to approximately 20 mL of distilled water, dissolved with the aid of a magnetic stirrer and hot plate, and the volume made up to exactly 30 mL only after complete dissolution, to avoid the volume error introduced by dissolving the solid directly in a pre-measured 30 mL of water. Table 2 lists the concentrations used and their measured refractive indices.

Table 2. NaCl solution concentrations and corresponding refractive indices.

NaCl concentration (%)	NaCl mass (g / 30 mL)	Refractive index
0.00	0.0	1.332
0.02	0.6	1.337
0.10	3.0	1.346
0.16	4.8	1.351
0.20	6.0	1.361

4.4 Light source

POF exhibits minimum attenuation (< 200 dB/km) in the wavelength windows 470–620 nm and 640–670 nm. A suitable source must additionally operate at low voltage (for safety in an aqueous environment), remain wavelength- and intensity-stable over long monitoring periods, and couple efficiently into the POF. Gas lasers (e.g. He–Ne) meet the optical requirements but are costly, require high-voltage supplies and are unsuited to wet environments, whereas semiconductor laser diodes (LDs) are inexpensive, compact, low-power, and offer lifetimes exceeding 100,000 h. A Class 1 LD (wavelength 670 nm, output < 1 mW) was therefore identified as a safe, low-cost option compatible with the POF attenuation windows [5]; in the present experiment a broadband white-light source was used to record the full transmitted spectrum for characterisation purposes.

4.5 Experimental set-up

The declad POF probe was connected at one end to a white-light source and at the other end to a spectrograph. The NaCl solution under test was applied to the exposed core region (the decladding cavity), and the transmitted spectrum was

IJIREEICE ISSN (O) 2321-2004, ISSN (P) 2321-5526
International Journal of Innovative Research in Electrical, Electronics, Instrumentation and Control Engineering
Impact Factor 8.021 ∺ Peer-reviewed & Refereed journal ∺ Vol. 14, Issue 6, June 2026
DOI: 10.17148/IJIREEICE.2026.14639

recorded and analysed using Avantes spectroscopy software, giving the variation of transmitted intensity with wavelength for each analyte refractive index.

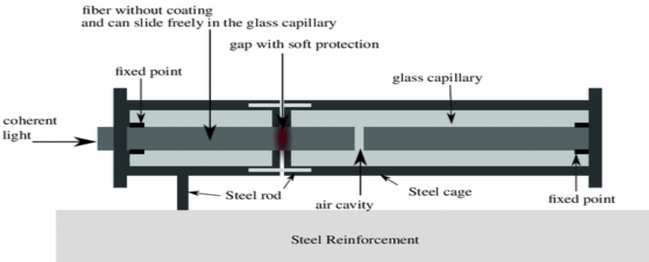

Fig. 2. Fixture used to clamp and declad the plastic optical fibre before sensing measurements.

5. RESULTS AND DISCUSSION

Transmitted intensity spectra were recorded for the declad POF probe in contact with each of the five NaCl solutions (RI 1.332–1.361). Representative spectra are shown in Fig. 3.

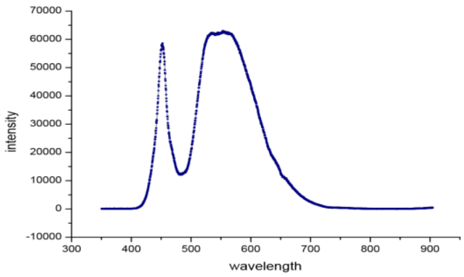

(a)

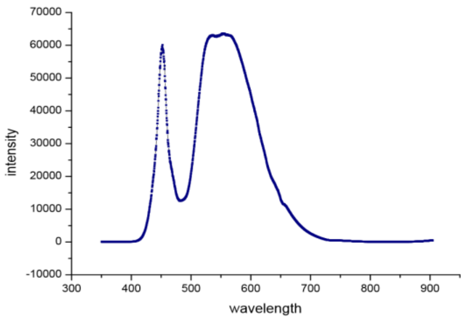

(b)

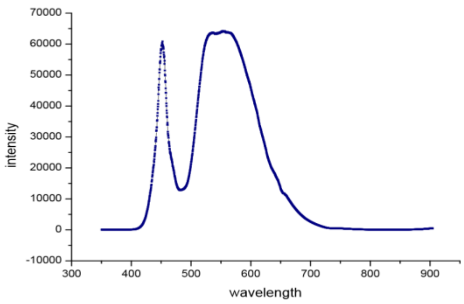

(c)

Fig. 3. Representative intensity vs. wavelength spectra of the declad POF probe in contact with NaCl solutions of refractive index (a) 1.332, (b) 1.346, and (c) 1.361.

 This work is licensed under a Creative Commons Attribution 4.0 International License

International Journal of Innovative Research in Electrical, Electronics, Instrumentation and Control Engineering
Impact Factor 8.021 ⁝⁝ Peer-reviewed & Refereed journal ⁝⁝ Vol. 14, Issue 6, June 2026
DOI: 10.17148/IJIREEICE.2026.14639

The peak transmitted intensity extracted from the spectra for each refractive index is summarised in Table 3.

Table 3. Peak transmitted intensity as a function of solution refractive index.

Refractive index	Peak intensity (a.u.)
1.332	62,400
1.337	62,800
1.346	63,180
1.350	63,400
1.360	63,740

The sensitivity of the probe, defined as the change in transmitted intensity per unit change in refractive index (counts/RIU), was calculated between successive concentration pairs and is reported in Table 4.

Table 4. Sensitivity of the declad-POF probe between successive refractive-index pairs.

Refractive-index pair	Sensitivity (counts/RIU)
1.332–1.337	80,000.0
1.337–1.346	42,222.2
1.346–1.350	55,000.0
1.350–1.360	340,000.0

The transmitted intensity increases monotonically with the refractive index of the surrounding solution over the entire range tested, and the sensitivity is markedly highest (3.4×10^5 counts/RIU) in the interval 1.350–1.360, closest to the refractive index of the POF cladding it replaces. This behaviour is consistent with evanescent-field theory: as the refractive index of the external medium approaches that of the fibre core, a larger fraction of guided power couples back into the core rather than leaking away, increasing the transmitted intensity and the sensitivity of the probe [2,7]. The increase may also be described in terms of a fibre non-linearity in which the propagation characteristics become a function of optical power, or equivalently of an increase in the effective refractive index of the waveguide; under such conditions the pulse-propagation characteristics of the fibre are modified and new frequency components can be generated, so that the output spectrum no longer replicates the input spectrum. Because the efficiency of this non-linear process scales with optical intensity and interaction length, it can be observed in an optical fibre at optical powers of only a few tens of mW, far below the powers normally required to observe non-linearity in bulk media [14].

NaCl solutions were selected as a stable, reproducible refractive-index standard because they were found to reproduce the intensity response obtained when a biofilm of Pseudomonas aeruginosa is grown directly on the exposed POF core, indicating that the present RI-based characterisation is directly transferable to a biological sensing configuration [2].

Looking beyond the present refractive-index characterisation, the broader field of optical-fibre sensing continues to advance through complementary strategies that could further enhance the performance of the present platform. Surface-plasmon-resonance configurations employing plasmonic metals and semiconductors such as thallium bromide and silicon carbide have been shown to extend the sensing range and improve the figure of merit of fibre-coupled plasmonic sensors [15,17]. Selective, label-free detection of specific analytes such as organophosphate pesticides has been demonstrated using MoS_2-coated planar polymer waveguides operating on a common-path interferometric principle [16], and more recently using molecularly-imprinted-polymer-coated optical fibres combined with machine-learning-assisted signal analysis [20]. In parallel, theoretical modal and dispersion analyses of engineered guiding structures such as Bragg fibres with asymmetric or reduced-cladding boundaries [18,19] point toward waveguide designs that could be adapted to further tailor the evanescent-field interaction exploited in the present sensor.

6. CONCLUSION

A low-cost intrinsic evanescent-field sensor was realised by locally decladding a step-index plastic optical fibre and exposing its core to the surrounding medium. Using aqueous NaCl solutions as a controllable refractive-index analyte, the transmitted intensity was shown to increase with the refractive index of the medium, with a maximum sensitivity of

International Journal of Innovative Research in Electrical, Electronics, Instrumentation and Control Engineering
Impact Factor 8.021 ⁒ Peer-reviewed & Refereed journal ⁒ Vol. 14, Issue 6, June 2026
DOI: 10.17148/IJIREEICE.2026.14639

3.4×10^5 counts/RIU obtained between RI 1.350 and 1.360. Because the NaCl-solution response reproduces that of a bacterial biofilm grown on the same probe, the declad-POF configuration developed here provides a simple, reproducible and inexpensive platform for the future development of fibre-optic biosensors for biofilm and refractive-index-based biochemical monitoring.

REFERENCES

[1] G. Keiser, Optical Fiber Communication, second ed., McGraw-Hill International Edition, New York, 1991 (Chapter 2).
[2] Y.M. Wong, Optimising the Plastic Optical Fiber Evanescent Field Biofilm Sensor, PhD Thesis, Liverpool John Moores University, 2008.
[3] M.D. Marazuela-Lamata, M.C. Moreno-Bondi, Fiber-optic biosensors – an overview, Anal. Bioanal. Chem. (2002).
[4] K. Thyagarajan, Fundamentals of Fiber Waveguide Modes, Winter College, International Centre for Theoretical Physics, 2007.
[5] R. Feynman, R.B. Leighton, M. Sands, The Feynman Lectures on Physics, vol. 2, chapter 2.
[6] P.N. Patel, V. Mishra, A.S. Mandloi, Optical biosensors: fundamentals and trends, Tech. J., Sardar Vallabhbhai National Institute of Technology, Gujarat, 2010.
[7] S. Silva, P. Roriz, O. Frazao, Refractive index measurement of liquids based on microstructured optical fibers, Photonics (2014).
[8] U.V. Biradar, S.M. Dongargre, Refractive index of salt (NaCl) from aqueous solutions, Int. J. Comput. Math. Sci. 4 (2015).
[9] L. Bilro, N. Alberto, J.L. Pinto, R. Nogueira, Optical sensors based on plastic fibers, Sensors (2012), ISSN 1424-8220.
[10] J. Zubia, L. Casado, G. Aldabaldetreku, A. Montero, E. Zubia, G. Durana, Design and development of a low-cost optical current sensor, Sensors (2013), ISSN 1424-8220.
[11] Optical Fibers, Unit 5, Sri Venkateswara College of Engineering (lecture notes).
[12] S. Abrate, R. Gaudino, G. Perrone, Step-index PMMA fibers and their applications, in: POF Handbook, Chapter 7.
[13] M. Espinosa Bosch, A.J. Ruiz Sanchez, F. Sanchez Rojas, C. Bosch Ojeda, Recent development in optical fiber biosensors, Sensors 7 (2007) 797–859.
[14] G.P. Agrawal, Nonlinear Fiber Optics, third ed., Academic Press, San Diego, 2001 (Chapter 2).
[15] V. Kumar, S. Pal, V. Singh, B. Goyal, L.K. Awasthi, Y.K. Prajapati, On the feasibility of thallium bromide in long-range plasmonic sensing for enhancement of performance, IEEE Trans. Plasma Sci. 52 (9) (2024) 4598–4605.
[16] A. Upadhyay, C.S. Yadav, R. Maurya, G. Sharma, T.S. Singh, S. Kumar, et al., Experimental detection of chlorpyrifos by MoS2-coated planar polymer waveguide sensor utilizing common-path interferometric principle, Optik 276 (2023) 170668.
[17] S. Kumar, V. Gupta, G. Sharma, G.C. Yadav, V. Singh, Investigation of silicon carbide based optical fiber coupled surface plasmon resonance sensor, Silicon 8 (4) (2016) 533–539.
[18] Y.K. Prajapati, V. Singh, J.P. Saini, Modal analysis and dispersion curves of a Bragg fiber having asymmetric loop boundary, Prog. Electromagn. Res. 87 (2008) 117–130.
[19] V. Singh, B. Prasad, S.P. Ojha, Analysis of the modal characteristics of a Bragg fiber with a small number of claddings using a very simple analytical approach, Microw. Opt. Technol. Lett. 46 (3) (2005) 271–275.
[20] A. Mishra, R. Maurya, S. Prakash, C.S. Yadav, A. Upadhyay, R. Singh, et al., Machine learning-enhanced detection of chlorpyrifos using molecularly imprinted polymer-coated optical fibers, Talanta 286 (2025) 127539.

 This work is licensed under a Creative Commons Attribution 4.0 International License